Developmental Cell
Short Article

Uncoupling Sonic Hedgehog Control of Pattern and Expansion of the Developing Limb Bud

Jianjian Zhu,[1] Eiichiro Nakamura,[1,3,5] Minh-Thanh Nguyen,[1,3,4] Xiaozhong Bao,[1,3] Haruhiko Akiyama,[2] and Susan Mackem[1,*]
[1]Laboratory of Pathology, National Cancer Institute, Bethesda, MD 20892, USA
[2]Department of Orthopaedics, Kyoto University, Kyoto, 606-8507 Japan
[3]These authors contributed equally to this work.
[4]Present address: Department of Ophthalmology, University of Cincinnati, Cincinnati, OH 45267, USA.
[5]Present address: Department of Orthopedic Surgery, University of Occupational and Environmental Health, Kitakyushu, 807-8555 Japan.
*Correspondence: mackems@mail.nih.gov
DOI 10.1016/j.devcel.2008.01.008

SUMMARY

Sonic hedgehog (Shh), which regulates proliferation in many contexts, functions as a limb morphogen to specify a distinct pattern of digits. How Shh's effects on cell number relate to its role in specifying digit identity is unclear. Deleting the mouse *Shh* gene at different times using a conditional Cre line, we find that Shh functions to control limb development in two phases: a very transient, early patterning phase regulating digit identity, and an extended growth-promoting phase during which the digit precursor mesenchyme expands and becomes recruited into condensing digit primordia. Our analysis reveals an unexpected alternating anterior-posterior sequence of normal mammalian digit formation. The progressive loss of digits upon successively earlier *Shh* removal mirrors this alternating sequence and highlights Shh's role in cell expansion to produce the normal digit complement.

INTRODUCTION

Manipulation of Shh levels in both chick and mouse embryo limb buds has demonstrated a quantitative, dose-dependent requirement for Shh to regulate both digit type (specified anterior-posterior, digits 1–5 or d1–d5, thumb to pinky) and total digit number (reviewed by Zeller, 2004; Tickle, 2006). Models for digit patterning by Shh include the classic spatial morphogen gradient model and the more recent expansion-based temporal gradient model (Harfe et al., 2004; reviewed by Zeller, 2004; Tickle, 2006), which both predict that the highest cumulative levels (either spatial or temporal) of Shh specify the most posterior digit. Yet, other work indicates that the most posterior *Shh*-expressing cells (d5 progenitors) become refractory to Shh signals over time and are only transiently Shh dependent (Marigo et al., 1996; Platt et al., 1997; Ahn and Joyner, 2004). Prior genetic tests of models of Shh function have manipulated Shh dose by modifying expression levels and/or altering Shh lipid modification (Lewis et al., 2001; Chen et al., 2004; Li et al., 2006; Scherz et al., 2007). The temporal requirements for Shh signals during normal digit development have not been evaluated directly by genetic removal, but only with the pharmacologic agent cyclopamine (Scherz et al., 2007; Panman et al., 2006; Stopper and Wagner, 2007), which blocks signal transduction by all hedgehog ligands (reviewed by Beachy et al., 2004), conflating later effects of Shh on digit skeletal morphology with those of Ihh required for normal chondrogenesis.

We have determined the temporal dependence of digit specification on Shh using a tamoxifen-inducible Cre-deleter line to remove a conditional (floxed) *Shh* allele at defined times during limb development. We find that Shh is required only very early and transiently for digit patterning, but continuingly to ensure sufficient cell numbers to produce the normal complement of digits. Hence Shh plays dual and distinct roles in regulating digit identity and number that can be uncoupled temporally.

RESULTS AND DISCUSSION

Shh Activity Is Completely Removed by the *Hoxb6/CreER* Deleter Line

A transgenic *Hoxb6/CreER* mouse line expressing CreER^T under the control of a *Hoxb6* promoter (Schughart et al., 1991) was used to drive high-level tamoxifen-dependent Cre activity in limb bud mesenchyme, spanning the entire period of *Shh* expression in limb (~E9.5–E12 for forelimb, and E10–E12.5 for hindlimb) (Buscher et al., 1997; Platt et al., 1997; Lewis et al., 2001) (see also Figure S1 in the Supplemental Data available with this article online). Using the *Rosa26LacZ* reporter, substantial Cre-mediated recombination was evident just 8 hr following single-dose tamoxifen intraperitoneal injections ranging from E9.5 to E10.5, and was complete by 12 hr (E9.5 shown, Figure 1A). Cre recombinase was active in the posterior two-thirds of the forelimb and the entire hindlimb bud. When this Cre transgenic line was crossed with a previously described conditional knockout (floxed) *Shh* allele (Lewis et al., 2001), tamoxifen-induced *Shh* deletion prior to the onset of *Shh* expression in hindlimb bud (E9.5) resulted in a high frequency of *Shh* null phenotype in hindlimbs (~90%, 29/32; Table S1; e.g., Figure 1B), indicating that recombination of the floxed allele was efficient enough to reduce Shh activity below a functional threshold. Earlier onset of *Shh* expression may explain the low frequency of *Shh* null phenotype in forelimbs (2/14 limbs; Table S1), which more often developed two digits (e.g., Figure 1B).

To assess the efficiency of tamoxifen-regulated Cre deletion of *Shh*, transcript levels were checked at different times following

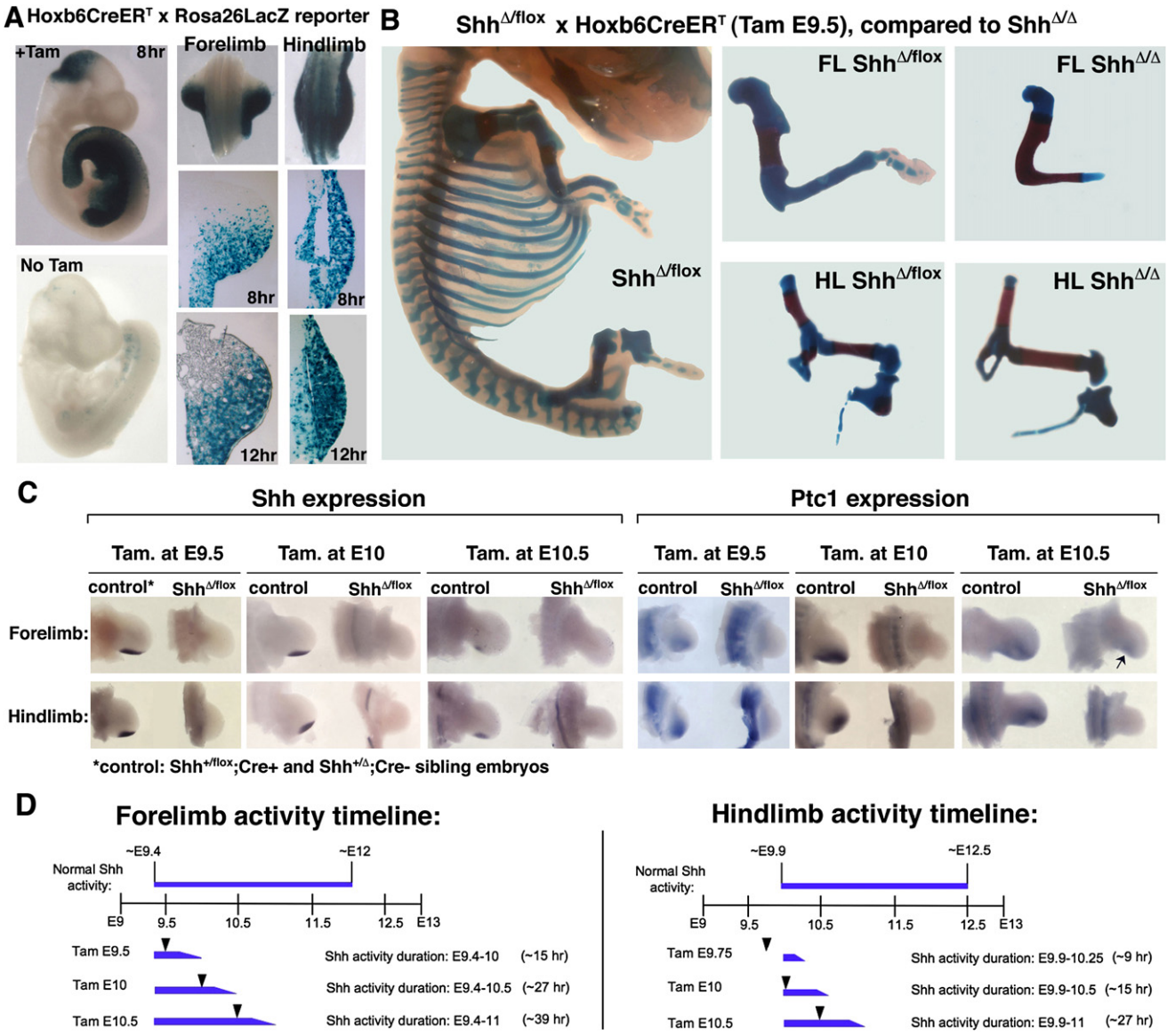

Figure 1. Efficacy of Recombination and *Shh* Removal Using a *Hoxb6CreER^T* Deleter Line

(A) *Cre+;LacZ* reporter-positive embryos show substantial recombination at 8 hr and essentially complete recombination by 12 hr after tamoxifen (Tam) injection.

(B) Tam-induced deletion of *Shh* prior to the normal onset of expression in hindlimb reproduces a null mutant phenotype.

(C) *Shh* (exon2-deleted) and *Ptc1* RNA are undetectable in limb buds at 18 hr after Tam-induced *Shh* removal. RNAs analyzed at both 18 hr and at 24 hr after each of the Tam injection times gave the same results. Examples shown were collected at 18 hr, except E9.5- and E10-treated *Shh*, and E10-treated *Ptc1*, which were at 24 hr. *Ptc1* transcripts were occasionally weakly detected in forelimb bud after Tam at E10.5 (arrow). Controls used were *Shh$^{+/flox}$;Cre+* and *Shh$^{+/\Delta}$;Cre−* sibling embryos; both showed similar *Shh* and *Ptc1* expression.

(D) Blue timelines summarize normal duration of Shh activity (*Ptc1* detection; see also Buscher et al., 1997; Platt et al., 1997; Lewis et al., 2001) and duration after Tam-activated Cre removal of *Shh*, based on a detailed time course of *Shh* and *Ptc1* expression (data from Figure S1) assayed at 3–5 hr intervals after different Tam injection times (marked by arrowheads).

tamoxifen treatment. *Shh* RNA was undetectable in both forelimb and hindlimb buds at 18–24 hr following tamoxifen treatment at either E9.5 (n = 11), E10 (n = 3), or E10.5 (n = 8) (e.g., Figure 1C). Since signaling molecules may function at very low levels, *Patched1* (*Ptc1*), a direct target of Shh (reviewed by Ingham and McMahon, 2001), mRNA levels were assayed to report residual Shh activity. *Ptc1* RNA was undetectable in most hindlimb buds within 18–24 hr following tamoxifen treatment at E9.5 (7/7), E10 (8/9), or E10.5 (8/9) (e.g., Figure 1C). In forelimb buds, *Ptc1* RNA was completely undetectable in ~50% of forelimb buds 18–24 hr after tamoxifen injection at E9.5 (4/8), E10 (5/9), or E10.5 (4/9), with only trace expression in the remainder (e.g., Figure 1C, arrow). These results show that tamoxifen injection eliminates Shh function in hindlimb buds and removes or reduces it to trace levels in forelimb buds. To delimit the window of Shh activity more precisely following tamoxifen injections at

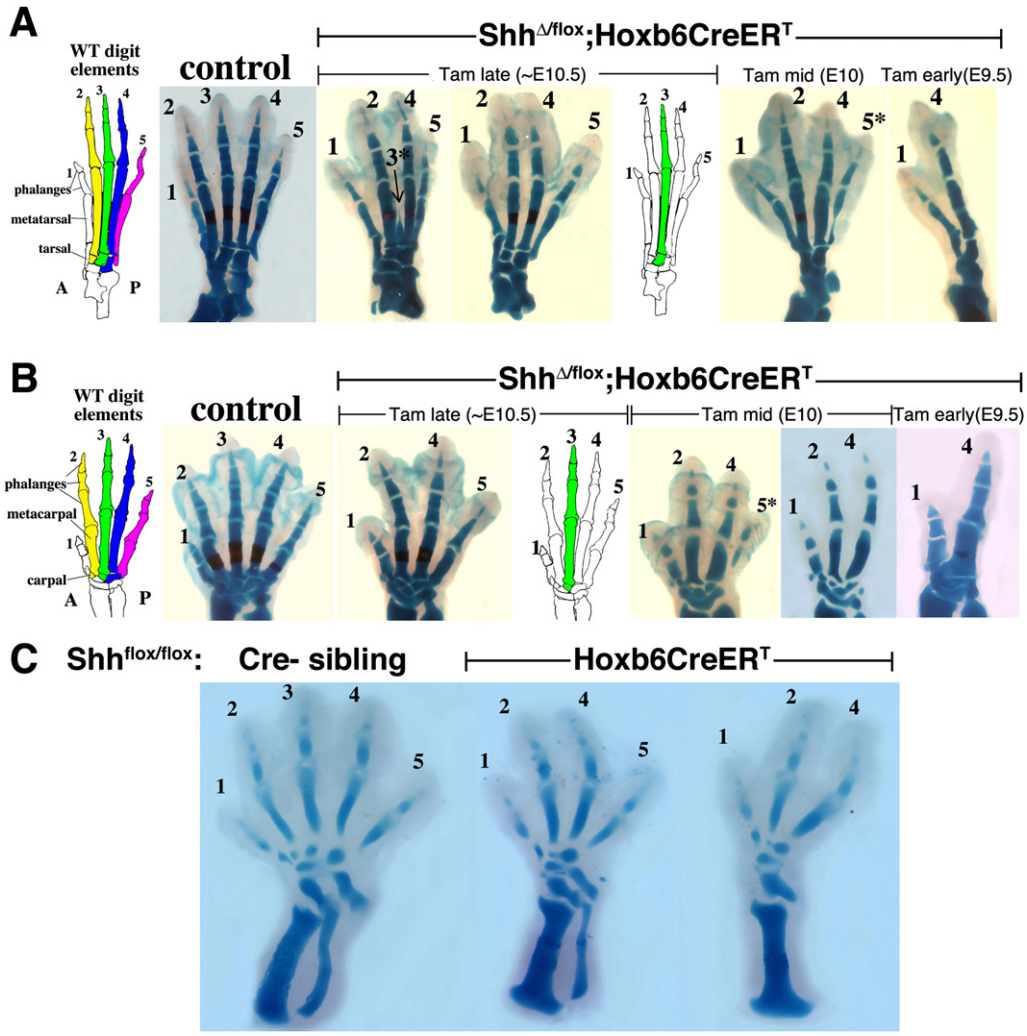

Figure 2. *Shh*$^{\Delta/flox}$;*Hoxb6CreER*^{T} Skeletal Phenotypes after Tam-Induced *Shh* Removal at E10.5, E10, or E9.5, with Progressive Loss of Digits d3, d5, d2, and d4

(A) Hindlimb skeletal phenotypes at E17.5 compared to sibling controls (as in Figure 1) at left, and schematic of wild-type limb skeleton showing different digits color-highlighted with their associated distal tarsal element, which was typically lost together with the overlying digit. Sometimes attenuated digits (asterisk) were observed prior to complete loss.

(B) Forelimb skeletal phenotypes at E17.5 (or E16.5 for E10 Tam) with controls and wild-type schematic showing carpals associated with specific digits.

(C) Hindlimb skeletons of E10 Tam-treated sibling embryos collected at E14.5, showing progressive loss of d3 followed by d5 at a very early skeletal stage, with unambiguous digit assignment based on very different initial tarsal sizes (note much larger size of the posterior-most tarsal in each case), and different lengths of d4 and d5. As the fibula is reduced or lost, the position of d4 and associated tarsal shift anteriorly to overlie the tibia.

each of the different times, *Shh* and *Ptc1* transcript levels were checked over a time course of the first 3–15 hr after IP tamoxifen injection (Figure S1). These data (summarized in Figure 1D) indicate that *Shh* transcripts are absent by ~5–6 hr after IP injection and that Shh activity is lost (based on *Ptc1* reporting) by ~12 hr after IP injection.

Tamoxifen-Induced *Shh* Removal at Successively Earlier Stages Does Not Perturb Digit Identity but Results in Progressive Digit Loss in the Sequence: d3, d5, d2, d4

We analyzed the digit skeletal phenotypes following a single tamoxifen injection at different times between E9.5 and E11 (e.g., Figure 2; summary, Table S1). As expected, progressively earlier injections elicited increasingly severe phenotypes (more digits lost). Determination of digit identity (see Experimental Procedures for criteria) was facilitated by the surprisingly normal digit morphologies in most of the embryos, even when only 2–3 digits remained; changes in number of phalanges were never observed. The order of digit loss was further confirmed by observed intermediate stages in which a clearly attenuated digit formed (asterisks in Figures 2A and 2B). Examination of 100 (each) fore- and hindlimbs revealed a highly consistent and unexpected order of digit loss: d3 first, d5 second, d2 third; leaving d4 as the last of the Shh-dependent digits (d2–d5) to be lost (e.g., Figure 2; summary, Table S2). This same sequence occurred in

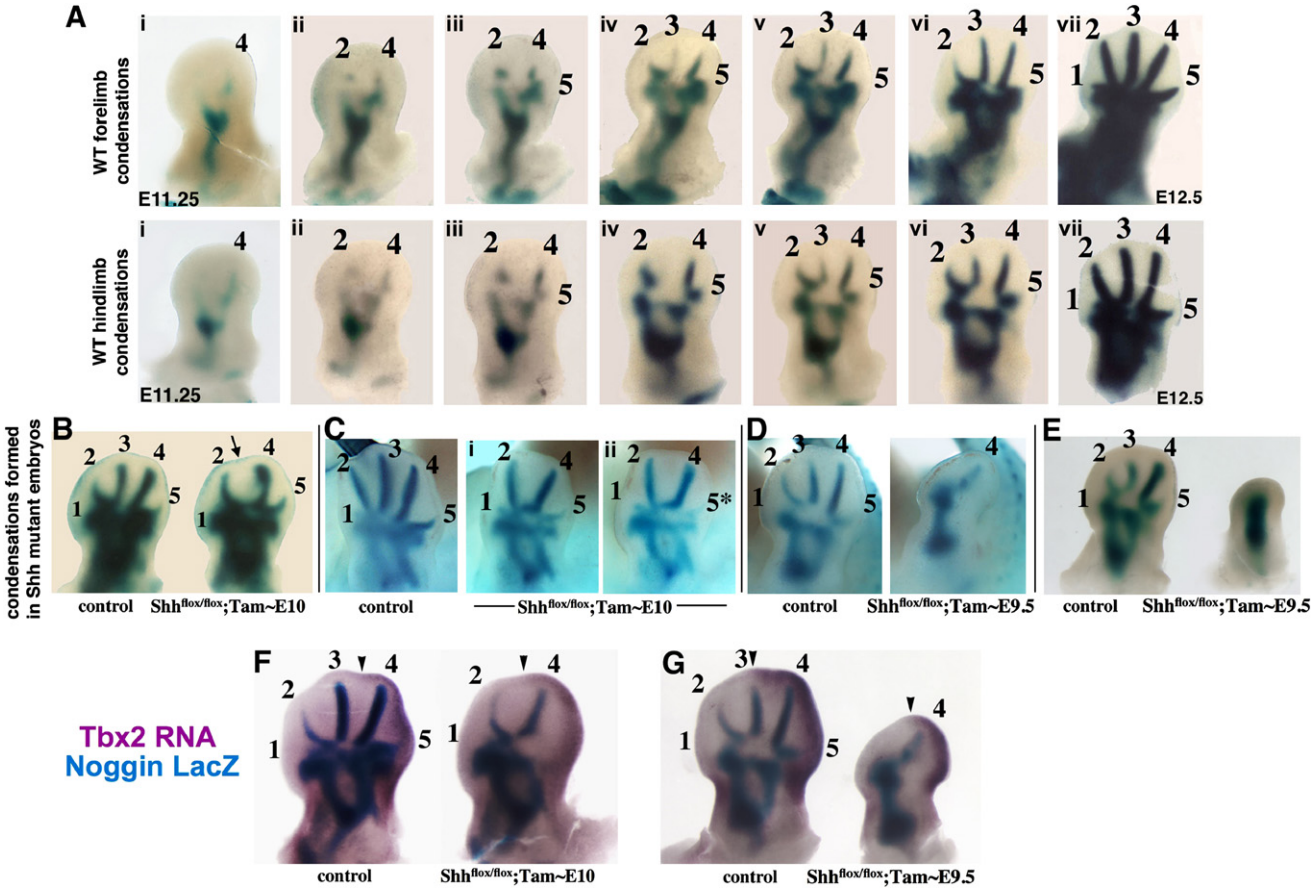

Figure 3. Formation of Digit Condensations in Wild-Type and *Shh*$^{flox/flox}$;*Cre*+ Embryos

(A) Normal condensation sequence of d4, d2, d5, d3 in fore and hindlimb buds visualized by LacZ activity in *Shh*$^{+/+}$;*Noggin*$^{LacZ/+}$ embryos at E11.25–E12.5. Digit 1 was not obvious in either wild-type or mutant condensations until very late (due to small size) and was not included in evaluating order.

(B–E) Condensation formation visualized by LacZ activity in *Shh*$^{flox/flox}$;*Cre*+;*Noggin*$^{LacZ/+}$ and control sibling (*Cre*−) limbs after tamoxifen given at the times indicated ([B] and [C] show forelimb; [D] and [E] show hindlimb). Note gap for d3 (arrow in [B]) and attenuated d5 (asterisk in [C]) upon progressively earlier *Shh* removal in mutants. The order of condensation loss was the same as in skeletal elements (Figure 2). In severer phenotypes, narrowing of the space between long bone condensations and conversion to a single condensation were also seen frequently ([D] and not shown).

(F and G) Double staining for posterior marker *Tbx2* and condensations (LacZ activity) in *Shh*$^{flox/flox}$;*Cre*+;*Noggin*$^{LacZ/+}$ embryos demonstrates *Tbx2* RNA (arrowheads mark anterior margin) in mesenchyme surrounding the distal posterior condensation of mutant embryos with two remaining digit precursors (F), and with a single, remaining long-digit precursor (G). In control siblings (Cre−), *Tbx2* RNA extends anteriorly up to d3 (arrowheads) but is completely absent from d2.

both fore- and hindlimbs. Assignment of the third digit lost (d2 versus d4) was more difficult than of the first two, because of fewer examples and the prior loss of adjacent skeletal landmarks. The last Shh-dependent digit was determined to be d4 based on the shape and size of the remaining carpal/tarsal bone, which is distinct from and larger than for d2, and on the proximal metatarsal shape, which has different joint morphology between d2 and d4, and was confirmed by analysis of posterior marker expression in mutant embryos at the earliest condensation stage (see below).

Wild-Type Digit Condensations Form in Reverse Sequence of Digit Loss upon *Shh* Removal

The unanticipated order of digit loss (d3, d5, d2, d4) following *Shh* removal is not predicted by any of the current spatial or temporal gradient models for Shh function in anterior-posterior patterning (reviewed by Zeller, 2004; Tickle, 2006). However, digit identity transformation superimposed upon digit loss could confound the simple interpretation of these results. There was no evidence at late skeletal stages (i.e., altered phalanx number or morphology) to suggest such transformations, and evaluation of very early skeletal phenotypes revealed the same sequence of digit loss as seen at later stages (Figure 2C). To further confirm that digit loss was unassociated with transformations in identity, phenotypes due to tamoxifen-induced *Shh* deletion were evaluated at the earliest stage that mesenchymal digit condensations first appear. *Noggin* is expressed very early in these condensations before cartilage differentiation markers (beginning at ~E11.25), and a *Noggin-LacZ* knockin allele (*Noggin*$^{LacZ/+}$) provides a very sensitive tool to detect these early condensations (Brunet et al., 1998).

Remarkably, the sequence of Shh-dependent digit condensation formation in wild-type mouse embryos, visualized with

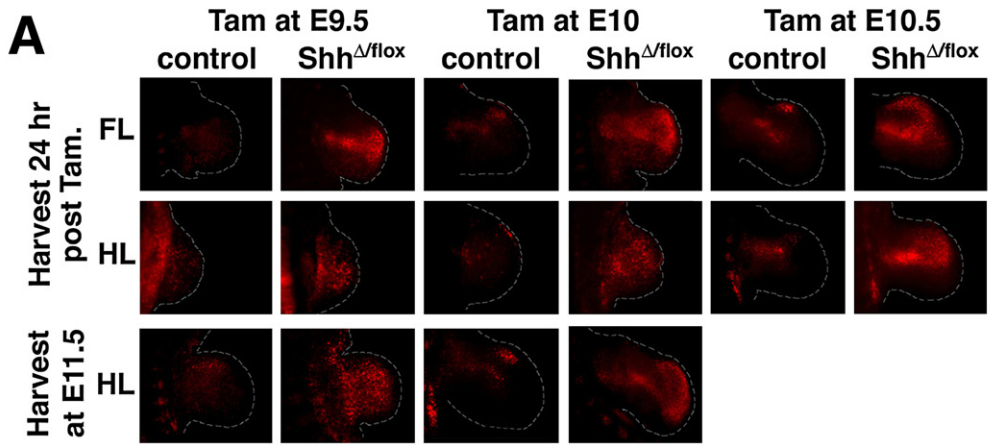

B

	Mitotic index measured at: E10.5	E11	E11.5
control	5.4 ± 0.4	3.7 ± 0.7	3.9 ± 0.6
24 hr after Tam: $Shh^{\Delta/flox}$	4.1 ± 0.5	3.3 ± 0.4	2.9 ± 0.8
36 hr after Tam: $Shh^{\Delta/flox}$			2.6 ± 0.6
48 hr after Tam: $Shh^{\Delta/flox}$			2.8 ± 0.6

C

	G1	S	G2/M
control	44.1%	39.8%	11.6%
$Shh^{\Delta/flox}$	54.8%	29.5%	11.3%

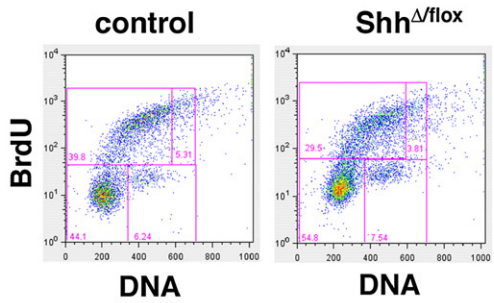

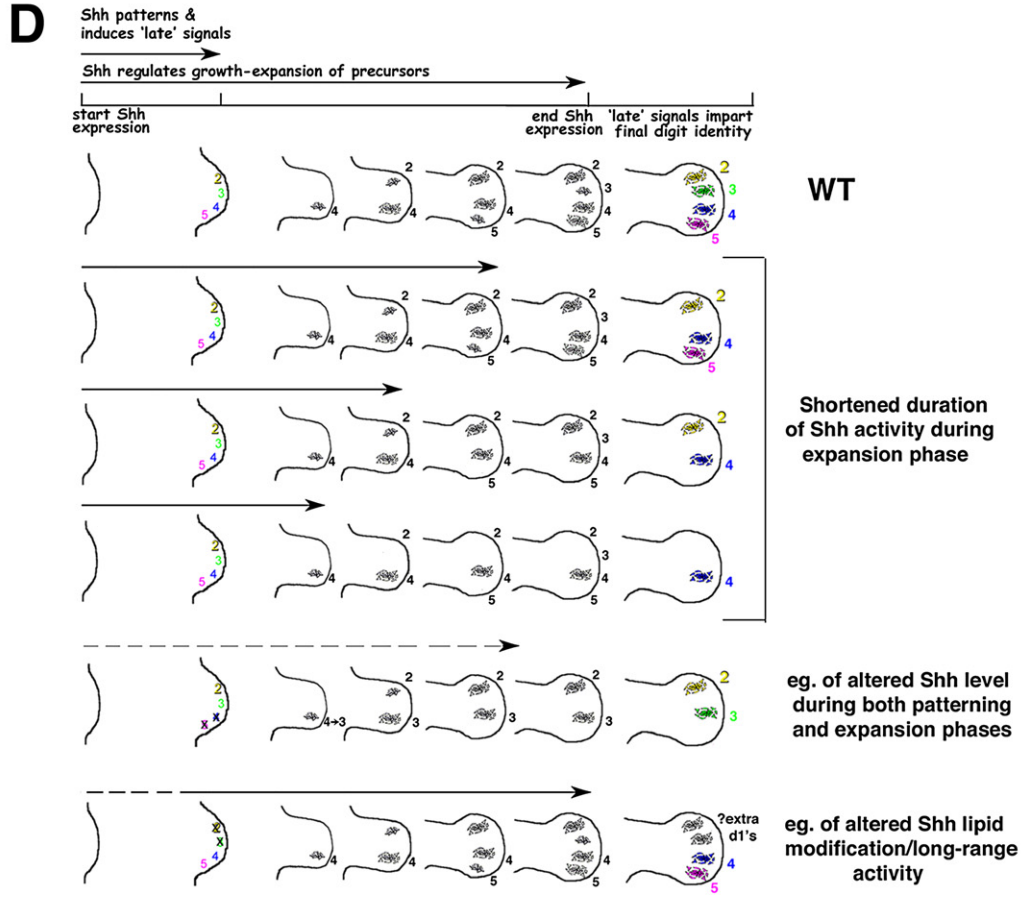

Noggin-LacZ, was d4,d2,d5,d3, exactly the reverse order of digit loss following *Shh* removal (Figure 3A; see also Figure S2). This order of normal mesenchymal condensation differs from that of their subsequent chondrogenic differentiation, which progresses in a more posterior-to-anterior order (Shubin and Alberch, 1986). *Sox9* is essential to form proper, stable mesenchymal condensations that undergo chondrogenic differentiation (Bi et al., 1999; Barna and Niswander, 2007) and is expressed slightly before *Noggin*. Although *Sox9* expression initiates weakly and almost synchronously in all digit condensations (making condensation order difficult to ascertain), a *Sox9-3′UTR-LacZ* knockin allele visualized early condensations and confirmed that digit 4 condensation appears first, then digit 2, followed by the rest in rapid succession (Figure S3). *Sox9* expression onset thus corroborated *Noggin* expression showing that digit mesenchymal condensations appear in a different order than the posterior-anterior progression of differentiation previously observed (i.e., d4, d2, d5, d3 rather than d4, d5, d3, d2). Whether an alternating AP mesenchymal condensation order occurs in other, nonmammalian tetrapods is not known; indeed, the order of appearance of differentiated chondrogenic condensations is not invariant between different tetrapods (Shubin and Alberch, 1986).

Digit Loss Following *Shh* Removal after the Onset of *Shh* Expression Is Not Associated with Transformations in Identity

Following tamoxifen-induced *Shh* removal, Noggin-LacZ-marked condensations revealed the same order of digit loss as observed later during skeletal stages (Figures 3B–3E), indicating that digit loss was unaccompanied by transformations in identity. The remaining single large condensation after early *Shh* removal (~E9.5; e.g., Figure 3D) was suspected to be d4 based on posterior swelling of the limb bud mesenchyme and the early appearance of this condensation in mutant limb buds at a time when only d4 had condensed in wild-type (data not shown). Expression analysis of the posterior marker *Tbx2* confirmed that the last remaining condensation following early *Shh* removal was d4 (Figures 3F and 3G). Although there are no known molecular markers that uniquely determine the identity of either d2 or d4, *Tbx2* expression at the condensation stage is restricted to the posterior mesenchyme surrounding the condensations of d4 and d5, whereas the mesenchyme surrounding d2 has no expression of this marker (Suzuki et al., 2004; Figure S2).

Because the normal number of condensations depends on the total available cell mass, when the mesenchymal cell population is reduced, fewer condensations form (reviewed by Mariani and Martin, 2003). Together, these results suggest that *Shh* deletion at all but the earliest stages (~E9.5, which gives a null phenotype in hindlimb) reduces cell number, and consequently fewer condensations form, but digit identity is still properly specified. In this case, recruitment of normal numbers of cells to the early-forming condensations yields morphologically normal digits, but cell depletion over time short-changes the latest-forming condensations. The attenuated digits observed at intermediate stages of digit loss (asterisks in Figure 2), support this view. Although it is impossible to judge whether or not absent digits were specified correctly (but simply failed to form), the persistence of d4 as the Shh-dependent digit that is least sensitive to *Shh* loss suggests that even very posterior digits (specified by high-level Shh activity) only require early, transient Shh function for correct specification (i.e., ~12 hr total of Shh activity, based on *Ptc1* expression; see Figure 1D and Figure S1). Though Shh activity is absent after ~12 hr, the blueprint for specifying different digit types is apparently preserved, suggesting there is simply insufficient material for making a normal complement of digits.

Shh Is Required Continuously to Maintain Cell Number for Limb Bud Expansion

Shh-related reduced cell number must reflect reduced proliferation and/or an increase in cell death at early stages in mutant limbs. Shh is a mitogen and a cell survival factor in many developmental systems and in cancer (reviewed by Ingham and McMahon, 2001; Beachy et al., 2004), and complete *Shh* removal during limb development (null mutant embryos) causes marked apoptosis of limb bud mesenchyme (Chiang et al., 2001). If changes in digit number following tamoxifen-induced *Shh* deletion are due to changes in cell number, then the severity of early cell reduction should parallel the severity of subsequent skeletal phenotypes. We evaluated apoptosis and proliferation levels in early limb buds following tamoxifen-induced *Shh* removal at different times. *Shh* deletion-induced apoptosis increased in spatial extent following progressively earlier tamoxifen treatment times (Figure 4A). Although slightly higher levels of apoptosis were noted in the anterior limb bud, there was no strict correlation between the spatial distribution of the apoptosis and the digit condensations lost. Mitotic cell indices were determined

Figure 4. Effect of Timed *Shh* Removal on Cell Survival and Proliferation

(A) Apoptosis (red fluorescence) in whole-mount forelimb (FL) and hindlimb (HL) buds of $Shh^{\Delta/flox}$;*Cre*+ embryos and control siblings (as in Figure 1) was analyzed at the ages indicated (left), following tamoxifen (Tam) injection at the times indicated (top). Dotted white lines indicate limb bud borders. Note the low level of increased apoptosis in $Shh^{+/flox}$;*Cre*+ embryos over $Shh^{+/\Delta}$;*Cre*− controls (*Cre*+ controls are shown for all E9.5 embryos), which was negligible compared to apoptosis in *Shh* mutants. By E11.5, apoptosis in mutant FLs (after Tam at E9.5 or E10) was declining (data not shown), but still prominent in HLs.

(B) Mitotic cell indices (mean ± σ) determined by anti-pH3 staining of *Shh* mutant and sibling controls (see Experimental Procedures and Figure S4).

(C) Cell cycle analysis of limb bud cells from *Shh* mutant and sibling controls at 24 hr after Tam at E10. Dot plots show bivariate flow cytometry analysis of BrdU/DNA-stained cells from sibling control (7,148 cells) or mutant (13,187 cells) embryos (1 hr BrdU pulse). G1 and S phase distributions were altered, but cell size indices were unchanged in *Shh* mutant compared to control limb cells (data not shown).

(D) Schematic showing dual roles of Shh in relation to formation of digit condensations, and to other signals regulating digit identity downstream of Shh. Digit 1, which is Shh independent (Chiang et al., 2001), is not shown. Panels below wild-type (WT) show phenotypes resulting when only the duration of Shh function is shortened during the expansion phase (this report), compared to quantitatively reduced Shh activity or altered Shh lipid modification during both phases. Condensations shown below different Shh-duration times (arrows) indicate the number of condensations ultimately forming after limb bud expansion, not already-formed elements.

using anti-phospho-histone H3 to stain cells in M phase (e.g., Figure S4). There was no statistically significant difference between *Shh* mutant and sibling controls 24 hr following tamoxifen treatment. However the mitotic index was slightly decreased in mutant compared to control hindlimb buds 36–48 hr after tamoxifen treatment, decreasing from a mean of 3.9% in controls to 2.6% and 2.8%, respectively, in the mutant limb buds ($p < 0.05$; see Figure 4B and Figure S4). The effect of *Shh* removal on proliferation appeared to be delayed relative to the time of onset of apoptosis; however, mitotic index is an insensitive reporter of cell cycle changes. To confirm altered proliferation after *Shh* removal by an independent method, limb buds from mutant and control embryos were dissociated and analyzed by flow cytometry to evaluate cell cycle parameters. Relative to controls, *Shh* mutant limb bud mesenchyme analyzed at 24 hr after tamoxifen injection showed an increase in the proportion of cells in G1 phase (54% versus 44%) and a decreased proportion entering S phase, consistent with a G1 cell cycle arrest in mutant limb buds (Figure 4C). Hence, removal of Shh activity alters both cell survival and proliferation in limb mesenchyme, and both effects may contribute to the resulting decreased cell number in mutant limbs.

Shh regulates cell survival, at least in part, indirectly by effects on apical ectoderm ridge (AER) maintenance (Litingtung et al., 2002; te Welscher et al., 2002; Michos et al., 2004; reviewed in Tickle, 2006). AER-Fgfs have been shown to be essential cell survival factors in the limb (Sun et al., 2002), and in fact, AER morphology and *Fgf8* expression are perturbed in the *Shh* null mutant (Chiang et al., 2001), which likely contribute to the altered cell survival observed. Indeed, after timed removal of *Shh* with tamoxifen, both the AER anterior extent and *Fgf8* expression level were reduced in mutant limb buds relative to controls after 24–36 hr (Figure S5), indicating that modulated AER maintenance may contribute to the observed changes in cell survival. However, loss of AER-Fgf function does not appear to directly alter cell proliferation (Sun et al., 2002); the cell cycle effects of Shh are likely mediated independently, via regulation of other targets in the limb.

A Biphasic Model for Shh Function in the Limb

Altogether, the results suggest an ongoing need for Shh to ensure adequate cell numbers for subsequent condensation and digit formation, by regulating both cell survival and proliferation. *Shh* removal may reduce total cell number proportionate with the duration of Shh absence so that the extent of digit loss is directly related to the timing of tamoxifen-induced *Shh* removal. If *Shh* removal at later times leaves AP patterning (digit identity specification) unperturbed, then the digits that still form would remain morphologically normal despite the cell number reduction, as we observed. The progressive loss of cells and of consequent digit number, with preserved identities of the remaining digits, together with digit loss in the reverse order that normal digit primordia condense, are most parsimoniously explained by a model in which Shh acts early and transiently to specify digits properly, and thereafter is required mainly to regulate cell numbers (see Figure 4D). The results do not negate a role for Shh in specifying different digit identities and conferring AP polarity, but these critical activities must be confined to a narrow window of early limb development when *Shh* is first expressed. Previous genetic fate mapping showed that d3 partly, and d4–d5 completely derive from cells that previously expressed *Shh* (Harfe et al., 2004), leading to a model for Shh patterning by signal integration over time. Our results are more compatible with Shh acting very early as a spatial morphogen or trigger. Although d4 and d5 normally derive from *Shh*-expressing precursors, maintenance of this expression over time is not essential for their specification per se, suggesting that the normal order of condensation formation also does not require Shh.

The finding that loss of Shh during the "expansion" phase reduces digit number without altering identities of remaining digits supports the view that digit identity is in fact determined at a very early stage, in so far as Shh requirement is concerned. However, there is also evidence that Shh may act in part through secondary signals (Yang et al., 1997; Drossopoulou et al., 2000) and that interdigit signals downstream of Shh function to regulate digit identity at late stages (Dahn and Fallon, 2000), thus relaying the patterning function of Shh beyond the time period of direct Shh activity. Our data do not contradict a contribution of late signals acting downstream of Shh, but rather suggest that the signal relay is set in motion during the earliest phases of Shh action (Figure 4D). Indeed, the action of late signals regulating identity would provide one mechanism for maintaining normal digit identities when reduced cell numbers become allocated into fewer condensations following later *Shh* removal. Alternatively, normal digit identities could be maintained in the face of reduced cell number if early digit condensation precursors were expanded at different times. However, there is currently no evidence for differential spatial proliferation zones in the limb bud as required by this model (Hornbruch and Wolpert, 1970; this report).

In previous studies where genetic manipulation of Shh lipid modifications and/or expression levels in mouse embryos produced partial digit loss (Lewis et al., 2001; Chen et al., 2004; Li et al., 2006; Scherz et al., 2007), the engineered alterations commenced immediately upon *Shh* expression onset. Thus, both early (digit identity specification) and late (control of digit number) Shh functions were simultaneously altered, resulting in different patterns of digit loss than we observed (Figure 4D). The same argument can be made for *Wnt7a* null mutant phenotypes, in which abnormal regulation of *Shh* results in highly attenuated *Shh* expression early (Parr and McMahon, 1995). In the only prior analysis of genetic *Shh* removal after expression-onset, *Shh* loss was evaluated at a single embryonic time point using a *PrxCre* line. *PrxCre* expression begins very early in prelimb mesenchyme (~E9; Hasson et al., 2007), yet *Shh* transcripts were not completely lost until much later (E11; Scherz et al., 2007), making it likely that Shh activity was reduced during both early patterning and later expansion phases. The resulting phenotype, with three digits usually remaining, has been variously interpreted as either d1, d2, d3 (Lewis et al., 2001; Scherz et al., 2007) or as d1, d2, d4 (Lewis et al., 2001). However, when the *Shh* expression level was reduced after onset (apparently without altered duration) using *ShhCre*, a single digit was lost, reported as d2 (Scherz et al., 2007). Distinction between d2 and d3 loss (in the absence of a phenotypic series with attenuated intermediates, as we have generated) is difficult. Notably, the late attenuation of *Shh* expression by genetic removal of *Fgfr1* also resulted in the consistent loss of just a single digit, reported as d3 (Verheyden et al., 2005).

The inhibitory drug cyclopamine has been used to evaluate the temporal requirements for Shh function, but results from such studies may be complicated by potential off-target effects and pharmacokinetic issues. For example, *Ihh* loss has striking effects on digit morphology (see Pacifici et al., 2005). In the chick, digit loss following cyclopamine was invariably associated with changes in digit identity (number of phalanges altered) as well as digit number, whereas we never observed phalangeal changes following genetic removal of *Shh* (Scherz et al., 2007). Whether this difference reflects the approach used or an inherent difference between birds and mammals remains to be seen. In mouse limb buds, cyclopamine's effects on gene expression were analyzed in short-term organ culture and showed that mid-phase 5′*Hoxd* expression recovered only slowly over time following drug-induced Shh inhibition (Panman et al., 2006), suggesting a prolonged requirement for Shh in regulating digit identity. 5′*Hoxd* genes play a role in regulating digit pattern downstream of Shh, but the timing of their functional requirement is still not established, and they may be required only very late following activation by other (as yet unknown) intermediaries downstream of Shh (reviewed by Mariani and Martin, 2003). Using timed removal of a floxed *Hoxd11-d13* allele (Zakany and Duboule, 1996), we have found that 5′Hoxd function is in fact essential after E11.5 for correct digit patterning; the phenotype resulting from tamoxifen-induced deletion at E11.5 is similar to the complete null phenotype (unpublished data). Furthermore, in the nonconditional *Shh* null mutant, although mid-phase *Hoxd* expression is absent in the limb, late-phase *Hoxd13* expression recovers completely in the hindlimb bud (and is clearly expressed by E11.5), indicating that late-phase *Hoxd* expression is *Shh* independent (Chiang et al., 2001).

Altogether, the data in this report provide strong support for the model that Shh, whether acting as a morphogen or trigger, specifies digit identity very early and that later, in the undifferentiated limb bud, Shh acts mainly to ensure sufficient cell numbers to form a normal five-digit limb. Mutant phenotypes attest to uncoupled growth in the face of absent or perturbed patterning (e.g., Litingtung et al., 2002; te Welscher et al., 2002); it is less clear whether the reverse, preserved patterning in the context of compromised growth, also holds. Our results suggest that patterning can in fact be uncoupled from growth. Such uncoupling of AP pattern from growth regulation may serve as one avenue for evolution to diversify and adapt digit number without disturbing normal digit morphology, as previously suggested (Shapiro et al., 2003; Stopper and Wagner, 2007).

EXPERIMENTAL PROCEDURES

Mouse Lines and Embryo Analyses

The *Shh*-floxed (Lewis et al., 2001), *Shh*-deleted (Chiang et al., 2001), and *Noggin/lacZ* knockin lines (Brunet et al., 1998) were described previously. The generation and characterization of the *Hoxb6/CreER*^{T} line will be described elsewhere (M.T.N. et al., unpublished data). All alleles were maintained on a predominantly FVB/n background, and expression profiles (in Figure 1D) are typical for this background. Somite numbers are also given for all intervals in detailed time course analyses (Figure S1). Noon on the date of the vaginal plug was defined as E0.5. Tamoxifen treatment (single IP dose of 3 mg), embryo collection, and analyses were described previously (Nakamura et al., 2006). A 246 bp *Shh* exon2 probe detecting only the floxed region was used to evaluate Shh transcript loss (generated with PCR primers 5′-GTGCAAAGAC AAGTTAAATGCCT-3′ and 5′-CAGTGGATGTGAGCTTTGGA-3′). Lysotracker (Molecular Probes) and anti-phospho-Histone H3 staining (Upstate Biotechnology) were used as recommended. $Shh^{flox/flox}$;*Cre*+ mice were mated with $Shh^{+/\Delta}$ or $Shh^{flox/flox}$ to generate mutant embryos with comparable results. Control siblings, including $Shh^{+/flox}$;*Cre*+ and $Shh^{\Delta/flox}$;*Cre*− genotypes (and in a few experiments, $Shh^{flox/flox}$;*Cre*−), and wild-type embryos had very similar gene expression, proliferation, and skeletal morphologies. $Shh^{+/flox}$;*Cre*+ embryos had slightly more apoptosis than *Cre*− controls. Mitotic indices were determined for control and mutant sibling embryos limb buds (Figure 4B) by counting pH3+/DAPI nuclei in the distal limb bud area (400–600 cells) on 3–4 stained sections from each of 1–3 independent limb buds of each genotype. Statistical significance of differences in average mitotic indices were determined using a two-tailed t test. For flow cytometry, 1 mg of BrdU was injected IP 60 min prior to embryo harvest; limb buds were dissected and dissociated (with 0.1% trypsin-EDTA, 1 mg/ml collagenase), and pooled forelimb or hindlimb pairs from an embryo were analyzed using a FITC-BrdU Flow kit (BD PharMingen) and FlowJo software.

Skeletal Analysis

E15.5–E17.5 embryos were processed and stained with alizarin red and alcian blue for skeletal analysis. Criteria used for assigning digit identity were: (1) importantly, loss of associated carpals or tarsals: for digits 2, 3, and 4, the shape and size of articulating wrist/ankle bones are distinctive (see diagrams in Figure 2) and were always lost together with the metapodial and phalangeal digit elements; (2) digit attenuation: often observed as an "intermediate" state (e.g., asterisks in Figure 2) that anticipated the next digit to be lost; (3) metapodial shape, particularly the proximal articular end; and (4) element length and timing of ossification, which were somewhat variable (even in wild-type and control siblings) and used mainly for secondary confirmation. Phalanx number is distinctive only for digit 1 and was not useful; all other digits normally have three phalanges, and loss of phalangeal elements was not observed in mutant embryos.

SUPPLEMENTAL DATA

Supplemental Data include five figures and two tables (detailed kinetic analyses of *Shh* and *Ptc1* expression decay following tamoxifen; *Tbx2* and *Tbx3* expression at normal two-digit condensation stage; Sox9-lacZ visualization of normal digit condensation order; mitotic levels and AER-*Fgf8* expression in mutant embryos; mutant phenotype frequencies and characteristics) and are available at http://www.developmentalcell.com/cgi/content/full/14/4/624/DC1/.

ACKNOWLEDGMENTS

We thank Cliff Tabin for stimulating discussions and comments on the manuscript, Richard Behringer and Rolf Zeller for critical reading of the manuscript, Mike Lenardo for insightful advice on key experiments, Seth Finger for assistance in assay development, Heiner Westphal and Chin Chiang for providing the *Shh* null allele mouse line, and Heinz Arnheiter for *Ptc1*, Benoit Bruneau for *Tbx2* and *Tbx3*, and Gail Martin for *Fgf8* probes. We also thank Andy McMahon for his generosity and service to the entire scientific community in making genetically engineered lines generated in his laboratory readily available to everyone. This research was supported by the Center for Cancer Research, National Cancer Institute, NIH.

Received: July 30, 2007
Revised: November 30, 2007
Accepted: January 18, 2008
Published: April 14, 2008

REFERENCES

Ahn, S., and Joyner, A.L. (2004). Dynamic changes in the response of cells to positive hedgehog signaling during mouse limb patterning. Cell *118*, 505–516.

Barna, M., and Niswander, L. (2007). Visualization of cartilage formation: insight into cellular properties of skeletal progenitors and chondrodysplasia syndromes. Dev. Cell *12*, 931–941.

Beachy, P.A., Karhadkar, S.S., and Berman, D.M. (2004). Tissue repair and stem cell renewal in carcinogenesis. Nature *432*, 324–331.

Bi, W., Deng, J.M., Zhang, Z., Behringer, R.R., and de Crombrugghe, B. (1999). Sox9 is required for cartilage formation. Nat. Genet. *22*, 85–89.

Brunet, L.J., McMahon, J.A., McMahon, A.P., and Harland, R.M. (1998). Noggin, cartilage morphogenesis, and joint formation in the mammalian skeleton. Science *280*, 1455–1457.

Buscher, D., Bosse, B., Heymer, J., and Ruther, U. (1997). Evidence for genetic control of Sonic hedgehog by Gli3 in mouse limb development. Mech. Dev. *62*, 175–182.

Chen, M.H., Li, Y.J., Kawakami, T., Xu, S.M., and Chuang, P.T. (2004). Palmitoylation is required for the production of a soluble multimeric Hedgehog protein complex and long-range signaling in vertebrates. Genes Dev. *18*, 641–659.

Chiang, C., Litingtung, Y., Harris, M.P., Simandl, B.K., Li, Y., Beachy, P.A., and Fallon, J.F. (2001). Manifestation of the limb prepattern: limb development in the absence of sonic hedgehog function. Dev. Biol. *236*, 421–435.

Dahn, R.D., and Fallon, J.F. (2000). Interdigital regulation of digit identity and homeotic transformation by modulated BMP signaling. Science *289*, 438–441.

Drossopoulou, G., Lewis, K.E., Sanz-Ezquerro, J.J., Nikbakht, N., McMahon, A.P., Hofmann, C., and Tickle, C. (2000). A model for anteroposterior patterning of the vertebrate limb based on sequential long- and short-range Shh signaling and Bmp signaling. Development *127*, 1337–1348.

Harfe, B.D., Scherz, P.J., Nissim, S., Tian, H., McMahon, A.P., and Tabin, C.J. (2004). Evidence for an expansion-based temporal Shh gradient in specifying vertebrate digit identities. Cell *118*, 517–528.

Hasson, P., Del Buono, J., and Logan, M.P.O. (2007). Tbx5 is dispensable for forelimb outgrowth. Development *134*, 85–92.

Hornbruch, A., and Wolpert, L. (1970). Cell division in the early growth and morphogenesis of the chick limb. Nature *226*, 764–766.

Ingham, P.W., and McMahon, A.P. (2001). Hedgehog signaling in animal development: paradigms and principles. Genes Dev. *15*, 3059–3087.

Lewis, P.M., Dunn, M.P., McMahon, J.A., Logan, M., Martin, J.F., St-Jacques, B., and McMahon, A.P. (2001). Cholesterol modification of sonic hedgehog is required for long-range signaling activity and effective modulation of signaling by Ptc1. Cell *105*, 599–612.

Li, Y., Zhang, H.M., Litingtung, Y., and Chiang, C. (2006). Cholesterol modification restricts the spread of Shh gradient in the limb bud. Proc. Natl. Acad. Sci. USA *103*, 6548–6553.

Litingtung, Y., Dahn, R.D., Li, Y.N., Fallon, J.F., and Chiang, C. (2002). Shh and Gli3 are dispensable for limb skeleton formation but regulate digit number and identity. Nature *418*, 979–983.

Mariani, F.V., and Martin, G.R. (2003). Deciphering skeletal patterning: clues from the limb. Nature *423*, 319–325.

Marigo, V., Johnson, R.L., Vortkamp, A., and Tabin, C.J. (1996). Sonic hedgehog differentially regulates expression of GLI and GLI3 during limb development. Dev. Biol. *180*, 273–283.

Michos, O., Panman, L., Vintersten, K., Beier, K., Zeller, R., and Zuniga, A. (2004). Gremlin-mediated BMP antagonism induces the epithelial-mesenchymal feedback signaling controlling metanephric kidney and limb organogenesis. Development *131*, 3401–3410.

Nakamura, E., Nguyen, M.T., and Mackem, S. (2006). Kinetics of tamoxifen-regulated Cre activity in mice using a cartilage-specific CreER(T) to assay temporal activity windows along the proximodistal limb skeleton. Dev. Dyn. *235*, 2603–2612.

Pacifici, M., Koyama, E., and Iwamoto, M. (2005). Mechanisms of synovial joint and articular cartilage formation: recent advances, but many lingering mysteries. Birth Defects Res. C Embryo Today *75*, 237–248.

Panman, L., Galli, A., Lagarde, N., Michos, O., Soete, G., Zuniga, A., and Zeller, R. (2006). Differential regulation of gene expression in the digit forming area of the mouse limb bud by SHH and gremlin 1/FGF-mediated epithelial-mesenchymal signalling. Development *133*, 3419–3428.

Parr, B.A., and McMahon, A.P. (1995). Dorsalizing signal Wnt-7a required for normal polarity of D-V and A-P axes of mouse limb. Nature *374*, 350–353.

Platt, K.A., Michaud, J., and Joyner, A.L. (1997). Expression of the mouse Gli and Ptc genes is adjacent to embryonic sources of hedgehog signals suggesting a conservation of pathways between flies and mice. Mech. Dev. *62*, 121–135.

Scherz, P.J., McGlinn, E., Nissim, S., and Tabin, C.J. (2007). Extended exposure to Sonic hedgehog is required for patterning the posterior digits of the vertebrate limb. Dev. Biol. *308*, 343–354.

Schughart, K., Bieberich, C.J., Eid, R., and Ruddle, F.H. (1991). A regulatory region from the mouse Hox-2.2 promoter directs gene-expression into developing limbs. Development *112*, 807–811.

Shapiro, M.D., Hanken, J., and Rosenthal, N. (2003). Developmental basis of evolutionary digit loss in the Australian lizard Hemiergis. J. Exp. Zoolog. B Mol. Dev. Evol. *297*, 48–56.

Shubin, N.H., and Alberch, P. (1986). A morphogenetic approach to the origin and basic organization of the tetrapod limb. In Evolutionary Biology, *Volume 20*, M.K. Hecht, B. Wallace, and G.I. Prance, eds. (New York: Plenum Press), pp. 319–387.

Stopper, G.F., and Wagner, G.P. (2007). Inhibition of Sonic hedgehog signaling leads to posterior digit loss in Ambystoma mexicanum: parallels to natural digit reduction in urodeles. Dev. Dyn. *236*, 321–331.

Sun, X., Mariani, F.V., and Martin, G.R. (2002). Functions of FGF signalling from the apical ectodermal ridge in limb development. Nature *418*, 501–508.

Suzuki, T., Takeuchi, J., Koshiba-Takeuchi, K., Koshiba-Takeuchi, K., and Ogura, T. (2004). Tbx genes specify posterior digit identity through Shh and BMP signaling. Dev. Cell *6*, 43–53.

te Welscher, P., Zuniga, A., Kuijper, S., Drenth, T., Goedemans, H.J., Meijlink, F., and Zeller, R. (2002). Progression of vertebrate limb development through SHH-mediated counteraction of GLI3. Science *298*, 827–830.

Tickle, C. (2006). Making digit patterns in the vertebrate limb. Nat. Rev. Mol. Cell Biol. *7*, 45–53.

Verheyden, J.M., Lewandoski, M., Deng, C., Harfe, B.D., and Sun, X. (2005). Conditional inactivation of Fgfr1 in mouse defines its role in limb bud establishment, outgrowth and digit patterning. Development *132*, 4235–4245.

Yang, Y., Drossopoulou, G., Chuang, P.T., Duprez, D., Marti, E., Bumcrot, D., Vargesson, N., Clarke, J., Niswander, L., McMahon, A., et al. (1997). Relationship between dose, distance and time in Sonic Hedgehog-mediated regulation of anteroposterior polarity in the chick limb. Development *124*, 4393–4404.

Zakany, J., and Duboule, D. (1996). Synpolydactyly in mice with a targeted deficiency in the HoxD complex. Nature *384*, 69–71.

Zeller, R. (2004). It takes time to make a pinky: unexpected insights into how SHH patterns vertebrate digits. Sci. STKE *259*, pe53.